Photonic microwave-signal-mixing technique using phase-coherent orthogonal optical carriers for radio-over-fiber application

Jianyu Zheng,[1,2] Jing Wang,[2] Jian Yu,[2] Ming Zhu,[2] Ze Dong,[2] Xin Wang,[1] Ting Su,[2] Jianguo Liu,[1,*] Ninghua Zhu,[1] and Gee-Kung Chang[2]

[1]*The State Key Laboratory on Integrated Optoelectronics, Institution of Semiconductors, Chinese Academy of Sciences, Beijing 100083, China*

[2]*School of Electrical and Computer Engineering, Georgia Institute of Technology, Atlanta, Georgia 30332, USA*
Corresponding author: jgliu@semi.ac.cn

An optical-assisted microwave-mixing technique based on orthogonal and phase-coherent optical carriers is proposed and demonstrated. High-quality binary-phase-shift keying, amplitude-shift keying, and on–off keying microwave modulation at 20 GHz implemented in the optical domain have been tested. The ultra-high-bandwidth response of the proposed mixing device is also analyzed and compared. The phase stability of the photonic microwave signal in the radio-over-fiber system is improved by the proposed signal mixing technique.   © 2014 Optical Society of America

The proliferation of high-speed multimedia services has been driving demand for increasing access data rates in the emerging 4G Long Term Evolution Advanced and 5G wireless communication networks. The strength of combining wide-band, low-loss optical fiber transmission with integrated microwave photonics systems has led to a strong interest in developing radio-over-fiber (RoF) technologies. In such systems, optical fiber can be used to distribute the microwave signals with high frequency to remote base stations (RBSs) from the center station (CS) [1]. One of the main issues for the RoF system is how to "migrate" the high-speed analog signal, i.e., the data-carried microwave, into the optical domain in the CS. In principle, the microwave signal generated by electrical mixing could be applied to modulate the optical carrier (OC) directly for realizing the electrical-to-optical conversion. However, this method will be unavailable as the microwave signal works at a high frequency band (>40 GHz) due to the electrical bandwidth restriction of the electro-optical modulator (EOM). The optical-carrier-suppressed modulation could be used to mitigate the bandwidth limit of the modulator if the microwave includes an intermediate-frequency signal [2]. In doing so, it will waste a lot of spectrum and restrict the quantity of data that the microwave can carry. In order to steer clear of a bottleneck from the EOM's bandwidth, a frequency-mixing approach in the optical domain has been proposed and demonstrated in the past few years, with a pure photonic microwave signal, i.e., two OCs (λ_1 and λ_2) with coherent phase, emitted from the photonic microwave source mixing with the data via an EOM. There are two kinds of optical-assisted mixing techniques, as shown in Fig. 1. The straightforward modulation method displayed in Fig. 1(a) has not been adopted widely due to the fact that the phase modulation for the microwave cannot be realized [3]. In order to achieve the generation of a photonic microwave signal with more spectral-efficient vector modulation, the optical-assisted

microwave-mixing device described in Fig. 1(b) has been proposed and adopted extensively in the recently reported high-capacity RoF links [3–9]. In this method, one of the OCs provided by the photonic microwave source is filtered out and mixed with the data via the EOM. The phase and amplitude modulations of the microwave seem to be achieved, but the phase coherence between the OCs is damaged totally because they travel independently in the separated optical paths [3]. The random phase fluctuation between the OCs induces very large noise in the generated microwave [10]. Even though the complicated phase-estimation algorithm (PEA) based on digital-signal processing (DSP) has already been carried out to remedy this defect in the RBSs [4–9], the transmission performance of the RoF system is still difficult to improve remarkably. Moreover, the complicated DPS component used in coherent core transport networks is unsuitable for RoF-based optical and wireless access networks considering the cost and power consumption.
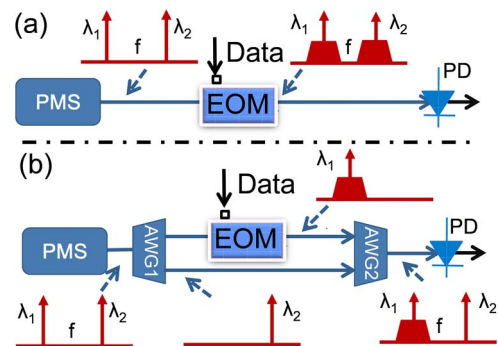

Fig. 1.   Schematic diagrams of the conventional optical-assisted microwave-mixing techniques. PMS, photonic microwave source; EOM, electro-optical modulator; AWG, arrayed waveguide grating; PD, photodetector. λ_1 and λ_2 are the wavelengths of the phase-coherent optical carriers (OCs) emitted from the photonic microwave source, and f is the frequency of the microwave generated by beating between the OCs.

In this Letter, an optical-assisted microwave-mixing technique is proposed and experimentally demonstrated. Because of the application of the orthogonal OCs with phase coherence, the random phase fluctuation between the OCs can be avoided in the processing of data modulation in the optical domain. The phase-stable binary-phase-shift keying (BPSK), amplitude-shift keying (ASK), and on–off keying (OOK) at 20 GHz microwave have been implemented in our experiment. The ultra-high bandwidth response for the proposed mixing device is also analyzed and demonstrated.

Figure 2 shows the schematic diagram of the optical-assisted microwave-mixing technique based on orthogonal OCs with phase coherence, the principle of which is stated as follows. A specially designed optical source, known as a phase-coherent orthogonal-light-wave generator (POLG), is used to provide two linearly polarized OCs λ_1 and λ_2 with matched phase whose states of polarization are orthogonal. The field of these orthogonal OCs is given by

$$\begin{bmatrix} E_{2,x}(t) \\ E_{1,y}(t) \end{bmatrix} = \begin{bmatrix} E_2 \cdot e^{j(2\pi f_2 + \varphi_0)} \\ E_1 \cdot e^{j(2\pi f_1 t)} \end{bmatrix}, \qquad (1)$$

where E_1 and E_2 are the original amplitudes of the OCs, f_1 and f_2 are the frequency of both OCs and equal c/λ_1 and c/λ_2 (c is the speed of light in vacuum), and φ_0 is the initial phase difference between the orthogonal OCs. As shown in Fig. 1, a polarization-sensitive EOM is applied to modulate the orthogonal OCs. Ideally, the property of the polarization-sensitive EOM is that the light traveling in the modulator will be modulated with maximum modulation efficiency (ME) while its polarization direction is parallel to the externally applied electric field (EAEF) but definitely will not be modulated while its polarization direction changes into the orthogonal direction. (The direction of the EAEF is defined as the y axis here.) Make sure that the polarization direction of the light λ_1 is parallel to the y axis as the orthogonal light waves enter into the ideal EOM. In this case, the modulated-light-wave output from the EOM could be expressed as

$$\begin{bmatrix} E_{2,x}(t) \\ E_{1,y}(t) \end{bmatrix} = \begin{bmatrix} E_2 \cdot e^{j(2\pi f_2 + \varphi_0)} \\ E_1(t) \cdot e^{j(2\pi f_1 t + \varphi(t))} \end{bmatrix}, \qquad (2)$$

where $\varphi(t)$ and $E_1(t)$ are the phase and amplitude modulations for the light λ_1. E_2 is the amplitude of the light λ_2. When the polarization direction of the light λ_1 is aligned at an angle of 45° to the principal axis of the polarizer, the optical field of the light waves after the polarizer could be written as

$$E_{45°}(t) = \frac{\sqrt{2}}{2}[E_1(t) \exp(j2\pi f_1 t + j\varphi(t))$$
$$+ E_2 \exp(j2\pi f_2 t + j\varphi_0)]. \qquad (3)$$

Clearly, after the polarizer, the polarization directions of modulated light λ_1 and unmodulated light λ_2 have been identical, and the photonic microwave mixing has already been completed. Even more importantly, the phase determinacy between the OCs λ_1 and λ_2 is never damaged in the whole process of frequency mixing due to the fact that these two light waves always travel in the same optical

path. Therefore, when the light waves are fed to the photo-detector (PD), the photocurrent could be presented as

$$I(t) \propto E_{45°}(t) \cdot E_{45°}^*(t)$$
$$= \frac{1}{2}(E_1(t))^2 + \frac{1}{2}E_2^2 + E_1(t)E_2 \cos(2\pi f t + \varphi_0 + \varphi(t)), \qquad (4)$$

where f is the frequency of the generated microwave signal, which equals $f_1 - f_2$. The data can be down-converted to the baseband by mixing with the pure microwave emitted from the electrical local oscillator. Then, data decision will be completed by DSP based baseband signal processing in the RBSs. Note that the DSP is simplified dramatically because the PEA does not need to be executed anymore. If the EOM shown in Fig. 2 is a LiNbO$_3$ Mach–Zehnder modulator (MZM), the BPSK microwave signal could be generated, as the MZM works at the minimum transmission point in the y axis. The ASK and OOK modulation could be implemented as the bias point of the MZM is increased gradually. There is no difference between the traditional electrical microwave mixer and the proposed mixing device in terms of the device's functions. It is evident that the core of the proposed mixing device is the POLG that is in charge of providing the orthogonal OCs with phase coherence.

There are several methods for generating orthogonal light waves with a matched and stable phase. Here, we choose a relatively simple method whose schematic diagram is displayed in Fig. 3. The light with a wavelength of λ_2 emitted from a laser diode (LD) enters a LiNbO$_3$ MZM whose polarization direction is oriented with the direction of the EAEF applied on the MZM at the angle α. The polarization rotator (PR) was fixed between the LD and the MZM, which consists of a quarter-wave plate and a rotatable polarizer. The angle α can be adjusted precisely by the PR. The asymmetry of the LiNbO$_3$ crystal induces
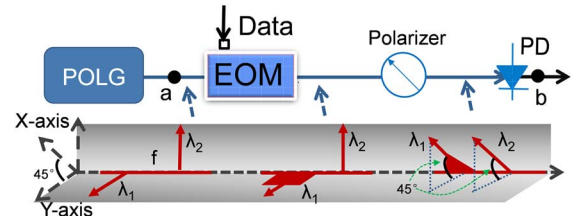

Fig. 2. Schematic diagram of the optical-assisted microwave mixer based on orthogonally phase-coherent lights. POLG, phase-coherent orthogonal-light-wave generator. Points "a" and "b" are the output ports of the POLG and the proposed mixing device, respectively.
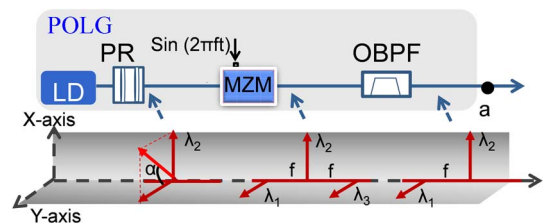

Fig. 3. Internal structure and schematic diagram of the POLG used in our experiment. PR, polarization rotator; MZM, Mach–Zehnder modulator; OBPF, optical bandpass filter. Point "a" is the output port of the POLG.

the change of the ME with the polarization direction of the injected light. Half-wave voltage in the axis with minimum ME, namely the x axis, is around 3.58 times of that in the y axis due to the electro-optical property of the LiNbO$_3$ crystal [11]. Therefore, while the component in the y axis of the injected light is modulated in the form of optical-carrier-suppression (OCS) by a microwave signal with a frequency of f, the modulation for the x-axis component of the light is insignificant. As shown in Fig. 3, $\pm$1st order optical side bands (λ_3 and λ_1) will be generated, and the OC will be suppressed in the y-axis direction. Meanwhile, the OC in the x-axis direction will be reserved. Ignoring the modulation and polarization-dependent loss (PDL) in the x axis, the optical field after the MZM could be expressed as

$$\begin{bmatrix} E_x \\ E_y \end{bmatrix} \approx E_0 \cdot e^{j2\pi \frac{c}{\lambda_2} t} \times \begin{bmatrix} \sin\alpha \\ \cos\alpha \cdot J_1(\beta) \cdot (e^{j2\pi f t} + e^{-j2\pi f t}) \end{bmatrix} \quad (5)$$

in the case of small signal modulation, where E_0 is defined as the original amplitude of the light, β is the modulation index, J_1 is the +1st order Bessel function of the first kind, and the operated wavelength of the LD equals λ_2. Thus, $\lambda_3 = \lambda_2 + c/f$ and $\lambda_1 = \lambda_2 - c/f$.

After the optical bandpass filter (OBPF), the OC in the x axis and the −1st order optical side band in the y axis, i.e., the orthogonal light waves λ_1 and λ_2, will be selected. The orthogonal light waves are phase coherent since they come from the same source. The power ratio between the orthogonal light waves could be controlled by adjusting the angle α. From Eq. (4), we can see the operational efficiency of the PD will be highest when the power ratio equals 1. The above-mentioned POLG was used to construct the proposed optical-assisted microwave-mixing device. In our experiment, all of the components were connected using the polarization-maintaining fiber (PMF). Moreover, in order to ensure the polarization direction of the light λ_1 is aligned with the principal axis of the polarizer at an angle of 45°, a specially designed polarizer was adopted whose principal axis aligns at an angle of 45° with the slow axis of the PMF in the input port.

Figures 4(a)–4(c) display the optical spectra of the modulated light before the OBPF when a 20 GHz microwave was applied on the inbuilt MZM. As expected, the OCS modulation was realized in the y axis, but the OC was reserved in the x axis [see Figs. 4(a) and 4(b)]. While α was set at 37° by adjusting the rotatable polarizer in the PR, the orthogonal light waves with power radio of 1 were generated by the POLG, as shown in Fig. 4(c). In this case, the optical signal was received and converted into electrical microwave signal via the PD, which was measured at point "b" in Fig. 1. The clear waveform of the frequency-beating microwave without carrying the data, shown in Fig. 4(d), proves that the phase coherence between orthogonal light waves λ_1 and λ_2 was not damaged, which is in accordance with the theoretical prediction.

As the 1 Gb/s nonreturn-to-zero pseudo-random bit sequence was applied on the MZM outside the POLG, the clear eye diagrams of the BPSK, ASK, and OOK modulation at 20 GHz was obtained by adjusting the bias point of the modulator [see Figs. 5(a)–5(c)]. After increasing the bit rate to 5 Gb/s, the proposed mixer could still work
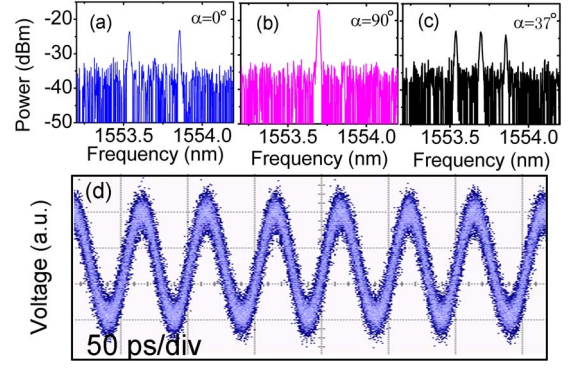

Fig. 4. (a)–(c) Optical spectra after the MZM in the POLG as the angle $\alpha = 0°$, 90°, and 37°. (d) Waveform of the unmodulated microwave with the frequency of 20 GHz recorded at point "b".

normally. Figure 5(d) shows the eye diagrams of a 5 Gb/s BPSK signal at 20 GHz. In fact, the modulation speed could be up to 40 Gb/s, which only depends on the modulation bandwidth of the modulator outside the POLG. In order to extend the operated frequency of the mixing device, the frequency spacing of the orthogonal light waves with phase coherence should be increased. In fact, according to the principle of the POLG described in Fig. 2, it is clear that the orthogonal light waves with 60 GHz frequency spacing can be obtained by using the third optical side band in the y axis as the power of the microwave applied on the MZM is increased.

Mixing the data with the electromagnetic wave works at the W-band or sub-THz is desired [3,4,7–9]. Therefore, we proposed an improved POLG that is illustrated in Fig. 6. Here, the optical comb generator (OCG) replaces the regular LD as the seed optical source. Because all of the combs are phase locked, the optical field of the optical combs could be expressed as

$$E(t) = \sum_m E_m \cdot e^{i2\pi \frac{c}{\lambda_m} t}, \quad (6)$$

where m is an integer and E_m and λ_m are the amplitude and wavelength of every optical comb, respectively:
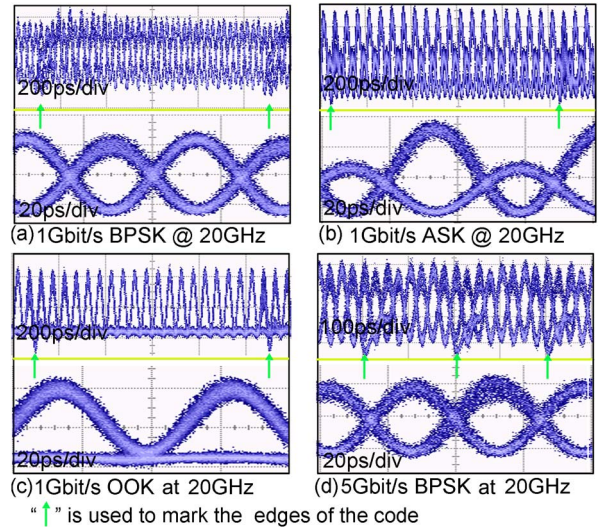

Fig. 5. (a)–(c) Eye diagrams of the 1 Gb/s BPSK, ASK, and OOK modulations at 20 GHz. (d) Eye diagrams of the 5 Gb/s BPSK at 20 GHz. All of them recorded at point "b".
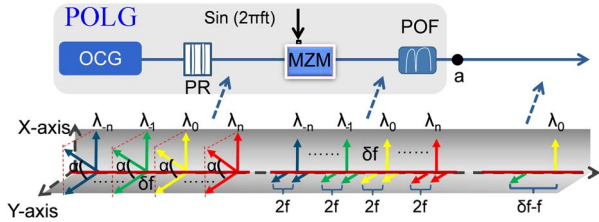
Fig. 6.   Internal structure and schematic diagram of the optical comb-based POLG. OCG, optical comb generator; POF, programmable optical filter. Point "a" is the output port of the POLG.

$$\lambda_m = \lambda_0 + m \cdot (c/\delta f), \qquad (7)$$

where λ_0 is the center wavelength of the optical combs and δf is the frequency spacing between the adjacent combs. Hence, as the microwave signal with the frequency of f is applied on the MZM in the POLG, Eq. (5) could be modified as

$$\begin{bmatrix} E_x \\ E_y \end{bmatrix} \approx \sum_m E_m \cdot e^{j2\pi \frac{c}{\lambda_m} t} \times \begin{bmatrix} \sin\alpha \\ \cos\alpha \cdot J_1(\beta) \cdot (e^{j2\pi f t} + e^{-j2\pi f t}) \end{bmatrix}. \quad (8)$$

It can be seen from Eq. (8) that the optical side bands of every comb are phase coherent with every comb. Hence, orthogonal OCs with sub-THz frequency spacing could be generated while one comb and one side band are selected properly by the programmable optical filter. [See the schematic optical spectra in Fig. 6.]

In principle, the phase-stable 4 or 16 quadrature amplitude modulation could be achieved if the EOM shown in Fig. 2 is a dual-parallel MZM rather than a regular MZM. Actually, the pilot tone vector modulator (PTVM) described in [12] is the optimal EOM for our proposed mixing device, which has the perfect polarization-dependent property. The frequency mixing for the base-band orthogonal-frequency-division multiplexing signals can be realized for further improving the capacity and spectrum efficiency of the PEA-free RoF system if the PTVM is used in the mixing device. Because of the application of the PMF, the light components λ_1 and λ_2 can be aligned with the x and y axes precisely as they enter the EOM. Therefore, the modulation cross talk is insignificant. Additionally, because α could be calculated precisely according to PDL (about 4 dB) and the half-wave voltage of the modulator and the peak-to-peak voltage of the electrical signal, the PR could be replaced by a PMF patchcord with a specially designed connector key in practice [10].

In conclusion, a phase-coherent orthogonal-light-wave-based optical-assisted microwave-mixing device is proposed and experimentally demonstrated. Phase-stable frequency mixing in the optical domain is realized for the first time. The BPSK, ASK, and OOK modulations at 20 GHz have been implemented. The theoretical analysis shows that the proposed mixing device could work at the sub-THz band if the OCG is used to generate the phase-coherent orthogonal light waves. Such findings are of great potential for applications in high-stability and low-cost RoF-based optical and wireless access networks.

References

1. C. C. Davis, I. I. Smolyaniov, and S. D. Milner, IEEE Commun. Mag. **41**, 51 (2003).
2. Z. Jia, J. Yu, and G. Chang, IEEE Photon. Technol. Lett. **18**, 1726 (2006).
3. T. Nagatsuma, S. Horiguchi, Y. Minamikata, Y. Yoshimizu, S. Hisatake, S. Kuwano, N. Yoshimoto, J. Terada, and H. Takahashi, Opt. Express **21**, 23736 (2013).
4. A. Kanno, K. Inagaki, I. Morohashi, T. Sakamoto, T. Kuri, I. Hosako, T. Kawanishi, Y. Yoshida, and K. Kitayama, Opt. Express **19**, B56 (2011).
5. L. Tao, Z. Dong, J. Yu, N. Chi, J. Zhang, X. Li, Y. Shao, and G.-K. Chang, IEEE Photon. Technol. Lett. **24**, 2276 (2012).
6. M. Zhu, L. Zhang, S.-H. Fan, C. Su, G. Gu, and G.-K. Chang, IEEE Photon. Technol. Lett. **24**, 1127 (2012).
7. L. Deng, M. Beltran, X. Pang, X. Zhang, V. Arlunno, Y. Zhao, A. Caballero, A. Dogadaev, X. Yu, R. Llorente, D. Liu, and I. T. Monroy, IEEE Photon. Technol. Lett. **24**, 383 (2012).
8. X. Li, Z. Dong, J. Yu, N. Chi, Y. Shao, and G. K. Chang, Opt. Lett. **37**, 5106 (2012).
9. S. Koenig, D. Lopez-Diaz, J. Antes, F. Boes, R. Henneberger, A. Leuther, A. Tessmann, R. Schmogrow, D. Hillerkuss, R. Palmer, T. Zwick, C. Koos, W. Freude, O. Ambacher, J. Leuthold, and I. Kallfass, Nat. Photonics **7**, 977 (2013).
10. J. Zheng, H. Wang, W. Li, L. Wang, T. Su, J. Liu, and N. Zhu, Opt. Lett. **39**, 1366 (2014).
11. M. Lawrence, Rep. Prog. Phys. **56**, 363 (1993).
12. A. Shahpari, R. S. Luis, J. D. Reis, R. M. Ferreira, Z. Vujicic, J. D. Mendinueta, M. Lima, N. Wada, and A. L. Teixeira, in *Optical Fiber Communication Conference*, OSA Technical Digest (Optical Society of America, 2014), paper W4G.1.